

**Conspicuous role of the neck-length parameter for future superheavy element discoveries**Sahila Chopra <sup>1</sup>, Peter O. Hess <sup>2,3</sup> and Manoj K. Sharma <sup>4</sup><sup>1</sup>Frankfurt Institute for Advanced Studies (FIAS), D-60438 Frankfurt am Main, Germany<sup>2</sup>Institute für Theoretische Physik, Goethe Universität, D-60438 Frankfurt am Main, Germany<sup>3</sup>Instituto de Ciencias Nucleares, UNAM, 04510 Mexico City, Mexico<sup>4</sup>School of Physics and Material Science, Thapar University, Patiala 147004, India

(Received 17 May 2023; accepted 18 July 2023; published 10 August 2023)

We brought to light the primordial importance and relevance of the neck-formation/neck-length parameter defined within the two center shell model, especially for the synthesis of new superheavy elements. We have implemented the quantum mechanical fragmentation theory in the dynamical cluster-decay model for the decay of a hot and rotating compound nuclear system. This theory provides a central idea to understanding the nucleus-nucleus collisions and the subsequent decay processes together such as fission and evaporation residue, etc. Our recently published result in the case of  $Z = 116$  and  $118$  has become a thrust of this work; we have successfully predicted the practical range of the cross sections of decay channels without tracing the experimental data. Henceforth, we can show that the neck-length parameter has a genuine power to predict the approximate cross section values for unknown decay channels. Such calculations may be useful for guiding experimentalists to choose adequate systems for the production of future superheavy elements

DOI: [10.1103/PhysRevC.108.L021601](https://doi.org/10.1103/PhysRevC.108.L021601)

*Introduction.* The search for new superheavy elements (SHE) continues to inspire contemporary nuclear physics research. Numerous theoretical studies have been performed and many more are being done, e.g., using the dinuclear system model [1–3], fusion-by-diffusion (FBD) model [4] based on the different set of parameters, and certain groups are working on the dynamical multidimensional stochastic (DMS) approach, based on Langevin equations. A few groups have performed promising work regarding light heavy-ion fusion reactions using the extended Hauser-Feshbach method (EHFM) [5]. An important point has been shown about the successful observation of missing charge distributions in heavy-ion reactions. Other studies [6] also worked for the predicted fission component in reactions involving lighter nuclei. These results make our work more convincing especially for the prediction of unobserved decay channels. In this Letter, within the framework of the dynamical cluster-decay model (DCM) [7–9], the important role of the neck-formation/neck-length parameter ( $\Delta R$ ) has specifically been defined. After getting recent results [10,11] based on the DCM approach, we are confident about the determined production rates in the case of SHEs, which may be considered for new experimental studies. A recent study in the cases of  $Z = 116$  and  $Z = 118$  [11] has proven that with the help of  $\Delta R$  we are able to predict the unexplored cross section values for the expected decay fragments. In these cases, our model predicted cross section values reproducing, with high precision, the experimental verified numbers. Here, on the basis of the  $\Delta R$  parameter, the DCM is shown to be a good contributor for future research for SHE. We work within the format of the DCM, based on a quantum mechanical description of the fragmentation theory (QMFT) [12–16], where a complete description of both fusion

and fission processes is achieved successfully by introducing two dynamical collective coordinates of mass ( $\eta_A$ ) and charge asymmetries ( $\eta_Z$  or  $\eta_N$ ) [15], within the asymmetric two center shell model (ATCSM) [16]. These two coordinates connect very well with the experiments and are an effective way to study heavy-ion reactions (HIR) because they help to account for the experimentally measured quantities, like yields and cross sections. QMFT has been successfully used to describe the dynamics of the compound nucleus in equilibrated as well as nonequilibrated exit channels. This theory provides a description for both cold and hot fission processes but even better for hot fission. In the DCM, preformation probability ( $P_0$ ) is a statistical quantity which sets this model apart from the other fission models. This factor explains the structure information about a compound nucleus during nuclear reaction and is able to suggest probable targets and projectiles in HIR for future synthesis of heavy and superheavy isotopes.

*The dynamical cluster-decay model based on fragmentation dynamics.* In this section we will briefly resume the DCM and its main characteristics. The DCM is an application of the QMFT based on the two center shell model (TCSM) [16]. As mentioned in the introduction, the unifying aspect of QMFT is to join two processes, i.e., nucleus-nucleus collision (fusion) and subsequent decay [fission/evaporation residues (ERs)]. This theory is used to select the appropriate projectile and target nuclei for the production of new elements. We are using this feature to make predictions for future discoveries in the case of new superheavy elements with the allowed range of the neck-length parameter ( $\Delta R$ ). This opinion will be helpful to demonstrate the significant role of the neck-length parameter in giving authentic values. In the QMFT, the collective

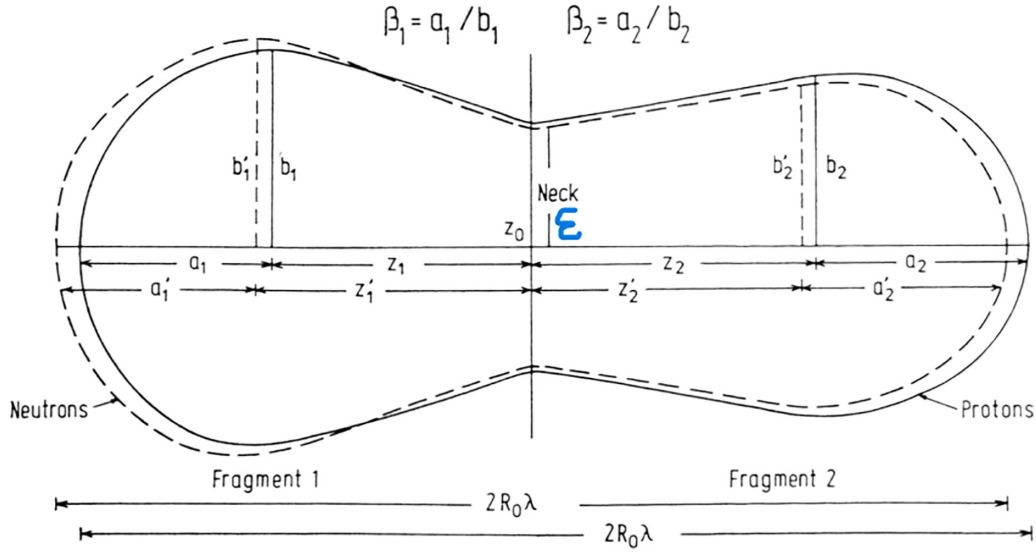


FIG. 1. A nuclear shape parametrized in the asymmetric two-center shell model for protons and neutrons (see Refs. [15,16]).

Hamiltonian is proposed as

$$H(\eta, R) = E(\eta) + E(R) + E(\eta, R) + V(\eta) + V(R) + V(\eta, R), \quad (1)$$

where the potential  $V$  is obtained using the Strutinsky method (based on an approximate liquid drop model [17] and the ATCSM [16]) by minimizing it in  $R$  and  $\eta$ . So far we have been using quantized motion in the mass and charge asymmetries and handled the relative motion classically.  $\eta_A$  and  $\eta_Z$  both define the nuclear reaction processes very well in ATCSM. In addition to these, the other commonly used coordinates are relative distance  $R$ , or, equivalently, length  $\lambda = \ell/2R_0$  ( $\ell$  is the total length of the system and  $R_0$  the radius of the corresponding spherical nucleus), deformation coordinates  $\beta_1$  and  $\beta_2$ , and neck coordinate  $\epsilon$  (see Fig. 1). The parameters  $\epsilon$ ,  $\beta_1$ ,  $\beta_2$ , and  $\eta_Z$  are determined by minimizing the potential energy (using the Strutinsky shell correction method [18]) for a given pair of  $R$  and  $\eta$  values. The important point to mention here is about the process on how minimization is performed within this methodology; i.e., for each compound nucleus, deep minima occur in the potential energy at only a few  $\eta$  values and these minima are not only stable in  $\eta$  but also no new minima appear after the two nuclei overlap to form a compound system.

Here, we are using the numerical solution of the stationary Schrödinger equation in the form of  $\eta_A$  or  $\eta_Z$ . In the first approximation, with the assumption that the coupling between  $\eta_A$  and  $\eta_Z$  is weak, we can take advantage of quantization in each of these coordinates separately and write the stationary Schrödinger equation as

$$H = -\frac{\hbar^2}{2\sqrt{B_{\eta\eta}}} \frac{\partial}{\partial \eta} \frac{1}{\sqrt{B_{\eta\eta}}} \frac{\partial}{\partial \eta} - \frac{\hbar^2}{2\sqrt{B_{RR}}} \frac{\partial}{\partial R} \frac{1}{\sqrt{B_{RR}}} \frac{\partial}{\partial R} + V(\eta) + V(R), \quad (2)$$

where  $\eta = \eta_A$  or  $\eta_Z$ . The value of  $R$  is fixed at the post-saddle point. Then, after proper evaluations, the mass or

charge distribution yields are given by  $|\psi_{R(\eta_Z)}(\eta_A)|^2$  or  $|\psi_{R(\eta_A)}(\eta_Z)|^2$ . Since  $\psi_R^{(\nu)}$  are the vibrational states in the potential  $V$ , in addition to  $\nu = 0$ , higher states with  $\nu = 1, 2, 3, \dots$  could also contribute. We consider these effects through a Boltzmann-like function

$$|\psi_R|^2 = \sum_{\nu=0}^{\infty} |\psi_R^{(\nu)}|^2 \exp(-E_R^{(\nu)}/T), \quad (3)$$

where  $T$  is the nuclear temperature and related to the excitation energy via

$$E^* = (A/a)T^2 - T \quad (\text{in MeV}) \quad (4)$$

with the level density parameter  $a = 11$  for SHE (for others  $a = 8-9$ ), depending on mass  $A$  of the compound nucleus (CN). Further, the DCM, extended to include deformation and orientation effects of the two incoming or outgoing nuclei, also contains the effects of angular momentum  $\ell$  and temperature  $T$ . Assuming that, in the entrance channel, a (excited) CN is formed with the CN fusion probability ( $P_{\text{CN}}$ ) equal to one, for all  $\ell$  partial waves, the CN decay or the fragments production cross section is

$$\sigma_{(A_1, A_2)} = \frac{\pi}{k^2} \sum_{\ell=0}^{\ell_{\max}} (2\ell + 1) P_0 P; \quad k = \sqrt{\frac{2\mu E_{\text{c.m.}}}{\hbar^2}}, \quad (5)$$

where  $P_0$  is the fragment preformation probability, referring to the  $\eta$  motion at fixed  $R$  value, and  $P$  the barrier penetrability to the  $R$  motion for each  $\eta$  value, both dependent on  $T$  and  $\ell$ . The details of our theoretical model are given in Refs. [10,11,19–23].

*Results and discussion.* Our group successfully studied many reactions forming light, heavy, and superheavy elements using the references of experimental data. For the last few years we have been noticing in our calculations that our model can identify the hidden/unobserved channels too, by calculating the realistic cross section values. The DCM is competent to evaluate the production probability with the assistance of

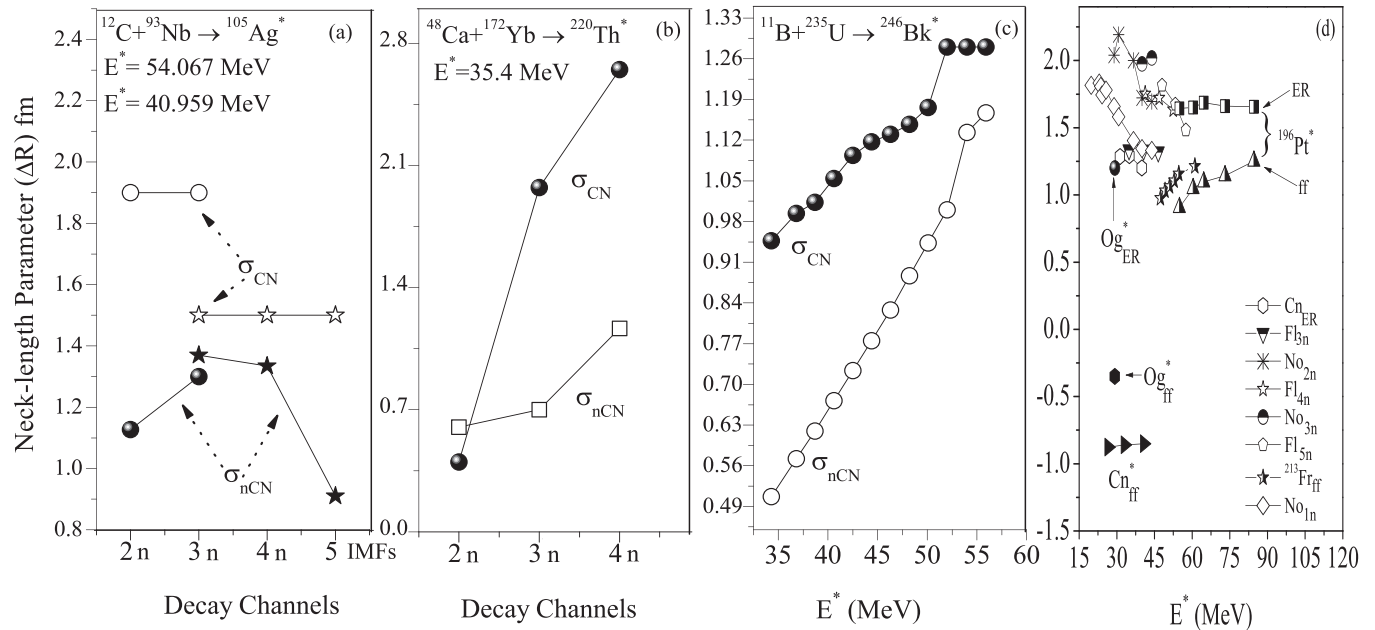


FIG. 2. Variation of neck-length parameter (a) for  $^{105}\text{Ag}^*$  [19] ( $E^* = 54.067$  MeV; star symbols and  $E^* = 40.959$  MeV; circular symbols), for individual decay channels. (b)  $^{220}\text{Th}^*$  [24] similar to (a) but showing the quality of the DCM for a different category of the mass regions. (c)  $^{246}\text{Bk}^*$  [25] with the variation of  $\sigma_{\text{CN}}$  and  $\sigma_{\text{nCN}}$  in the  $\sigma_{\text{fusion}}$ , and in (d) branch, we have shown a few nuclei, i.e., Pt\*, Og\*, Fl\*, Cn\*, No\*, and Fr\* governed via different decay channels (ER and ff). In the case of all studied compound nuclei the DCM calculations are in the agreement with experimental data. Specially, Pt\* [10] and Og\* [11] compound nuclei show a very good agreement, with a strong evidence of  $\Delta R$  ability to predict sensible cross sections for possible decay channels or predict the unobserved channels.

$\Delta R$ . In this work we share this feature of our model for the benefit of getting supportive ideas for the synthesis of new superheavy elements. The DCM predicts reasonable fusion cross sections and can propose promising projectile-target combinations.

*Neck-length parameter: how does it work?* In this Letter we have proposed the answer to a question: What is the importance of the neck-length parameter in the DCM? This parameter represents the clear probability of decay fragments breaking off from the compound nucleus during the decay process. Here, the neck-length parameter ( $\Delta R$ ) is the separation distance between surfaces of two fragments that assimilates deformation and neck formation effects between two nuclei. Figure 1 shows the explicit description for the concept of neck formation. When two decay fragments move away from each other during fission, a pull is created on them and a neck starts to form (along the  $z$  axis in Fig. 1). After fission, when the compound nucleus segregates into two separate fragments, the integration extends only to that point on the  $z$  axis where the fragments end; i.e., the potential becomes zero ( $V = 0$ ) when the decay fragments are not subjected to any forces. In the DCM,  $\Delta R$  is the principal parameter working in conjunction with the preformation ( $P_0$ ) and penetration ( $P$ ) probability. These parameters are directly related to each other and control the output of the DCM calculations very well. Every parameter has a real impact in the calculations. Using the proximity limit of  $\Delta R \approx 2$  fm, we are able to give the information of the mass dispersion potential  $V_{(\eta_A)}$  obtained from ATCSM. This procedure shows the potential energy minima (PES) for the possible target-projectile combinations. During

the decay processes all the fragments move under each other's influence up to the Coulomb range. This process can also be understood in the form of  $P_0$ . Note the preformation probability  $P_0$  is a quantum-mechanically normalized quantity; thus a small change due to one fragmentation will affect the yields of all remaining fragments. As long as the decay channels do not cross the barrier, they remain under each other's influence, so the distance ( $\Delta R$  value) of their exit will not be autonomous. This influence of  $\Delta R$  gives the approximate output of cross section values. Here, we are claiming to give a range of the neck-length parameter, within which achievable target to projectile (t-p) combinations can be found. This is a noticeable quality of the DCM, where all the decay fragments are treated on equal footing (simultaneously). This method is quite good to calculate the cross sections of known and unknown (but possible) decay fragments.

*Calculated results.* In almost all the DCM-based studies, including heavy and superheavy elements, calculated results are in good agreement with the experimental data (see Fig. 2). We have several pieces of evidence of the capability of  $\Delta R$  to address the nearly perfect cross section values for every single decay channel. This imparts useful inputs for assisting future discoveries and may be important for further experiments.

We note the following regarding the DCM-based calculations: The simultaneous observation of all decay fragments during the fission process strengthen this model with the capability to explain nuclear fragmentation within the framework of preformation probability ( $P_0$ ). The DCM is applicable for all mass regions as light to heavy and superheavy. In this Letter our main focus is on the synthesis of superheavy

discoveries and how  $\Delta R$  can be helpful for future experimental studies. In the cases where a compound nucleus is formed via permissive t-p combinations with a high percentage of  $P_{\text{CN}}$ ,  $\sigma_{\text{ER}}$  is found to be dominant. In that case,  $\Delta R$  will follow a trend:  $\Delta R$  increases systematically from ff to ER; i.e.,  $\Delta R$  is largest for ER (occurs first than ff), and smallest for the ff region. As, we know, the CN de-excites by evaporating nucleons (“fusion-evaporation”, or ER) or by fission (“fusion-fission” or ff). But the nuclear system can also re-separate before CN formation thus resulting in quasifission (qf) and/or capture and/or nCN. In the case of SHE, the capture cross section or total fusion cross section is then the sum of qf, ff and ER cross sections:  $\sigma_{\text{fusion}} = \sigma_{\text{qf}} + \sigma_{\text{ff}} + \sigma_{\text{ER}}$ , where the  $\sigma_{\text{fusion}} \approx \sigma_{\text{qf}}$ . For light nuclear systems,  $\sigma_{\text{fusion}} \approx \sigma_{\text{ER}}$ . But in very heavy (or SHE) systems the strong Coulomb repulsion and large angular momenta lead to tiny probabilities for CN formation and survival, and with this to the tiny values of  $\sigma_{\text{ER}}$ . This clears up the fact about the consequence of the small  $\sigma_{\text{ER}}$  (e.g., in pb for SHE), compared to  $\sigma_{\text{ff}}$  and  $\sigma_{\text{qf}}$  (in mb), leading to lower calculated CN formation probability ( $P_{\text{CN}}$ ). The higher cross section of ERs always gives the indication about the stability of the compound nuclei. However, an increase in the Coulomb repulsion between the interacting nuclei brings out the quasifission (qf) and deep inelastic processes, which firmly suppress the formation probability of the compound nucleus. In this work our main focus is on SHE discoveries, and our DCM result from [11] enabled us to move further with a trend of  $\Delta R$  (from ff to ER). With a considerable contribution of qf, the drift of  $\Delta R$  for qf will lie in between ER and ff. These results are also in agreement with earlier results for lighter- $Z$  superheavy nuclei [26,27]: the neck-length parameter increases systematically from ff to ER; i.e.,  $\Delta R$  is largest for ER, smallest for the ff region, and lies in between for qf. Note: we are not saying that this trend will remain for every element forward, but this trend may be possible for future SHEs. Different  $\Delta R$ 's (equivalently, relative separations) for the three processes predict that the processes ER, ff, and qf happen in different time-scales.

It should be clear that if any of the decay fragment is observable at a large distance ( $\Delta R$ ) it will occur more promptly than other consecutive decay channels in a nuclear reaction. Figure 1 demonstrates this fact via the neck formation, along the  $z$  axis when fragments move apart under the influence of the potential. At a specific distance ( $\Delta R$ ) they will become free from any type of pull and different  $\Delta R$  yield different cross section values. Figure 2 displays a description of the ability of the neck-length parameter to calculate the cross section of different decay channels (according to the defined mechanism as shown in Fig. 1, along the  $z$  axis). This parameter works very well not only for the CN cross sections ( $\sigma_{\text{CN}}$ ) of ER and ff but also for qf/nCN ( $\sigma_{\text{nCN}}$ ). In a single CN system, we may have a different percentage for CN and nCN contributions and  $\Delta R$  can help to address both. In this figure, we have made an effort to explain the effect of  $\Delta R$  for different compound nuclei, as panel (a) the CN  $^{105}\text{Ag}^*$  [19] shows the  $\Delta R$  values for  $2n$ ,  $3n$ ,  $4n$  channels and for intermediate mass fragments (IMFs;  $A_2 = 5-13$ ) to calculate the contribution of CN ( $\sigma_{\text{CN}}$ ) and nCN cross sections ( $\sigma_{\text{nCN}}$ ). It is very interesting that the calculated values we obtained are almost in accurate

agreement with the experiment. Here, the contributions of CN and nCN cross sections are obtained at different neck-length parameters. In Fig. 2(b), similarly as (a), the CN  $^{220}\text{Th}^*$  [24] have different decay channels ( $2n$ ,  $3n$ ,  $4n$ ) with very precise  $\Delta R$  values. This is a very sensitive parameter, and values for different decay fragments can easily affect each other's cross sections. So, simultaneous calculations are extremely necessary for good results. In (c), we present  $\Delta R$  for  $\sigma_{\text{CN}}$  and  $\sigma_{\text{nCN}}$  according to the contributed percentage to the total/fusion cross sections ( $\sigma_{\text{total}} = \sigma_{\text{CN}} + \sigma_{\text{nCN}}$ ). Here, the DCM shows the capabilities to calculate CN and nCN cross sections from the individual decay channels or from the total cross section at different excitation energies.

In this work, the most highlighted feature of the DCM is displayed in Fig. 2(d) with  $\Delta R$  to giving the predicted cross sections of unobserved decay channels. First, we have tried our new practice in the case of  $\text{Pt}^*$  [10]. With only the availability of  $\sigma_{\text{ER}}$ , we have predicted the corresponding  $\sigma_{\text{ff}}$  at a particular energy. In Fig. 2, the lower curve for  $\text{Pt}^*$  is shown as a particular trend, which clearly reveals the predicted number goes along with the other measured cross section values. This result is the foundation to predict the cross sections for unobserved decay channels. Using the same concept, we have calculated the cross sections in the case of  $Z = 116$  and  $118$  [11] without adjusting any experimental data. Here, it is worth noting that the realistic DCM-calculated results are significant for the existence of  $\Delta R$ . In panel (d), we have mixed contributions of  $\Delta R$  for ER and ff. Here, we did not consider the nCN contribution. However, an important point to note here is that the decay channels with the higher  $\Delta R$  show their main contribution in the compound nucleus formation probability  $P_{\text{CN}}$ . This figure also exhibited a comprehensible vision of this parameter to calculate the cross section of different decay channels according to their preformation probabilities. Along the  $y$  axis, we display six compound nuclei,  $\text{Pt}^*$ ,  $\text{Og}^*$ ,  $\text{Fl}^*$ ,  $\text{Cn}^*$ ,  $\text{No}^*$ , and  $\text{Fr}^*$  (see Refs. [10,11,26–29]), and all are in good agreement with experimental data which shows that the DCM calculations reproduce the experiments with great accuracy, whether they are evaporation residues or fission fragments.

*Summary and conclusions.* In conclusion, on the basis of this study, our expectation becomes even stronger for the potential of the neck-length parameter. Here, we have demonstrated the predictability of the neck-length parameter, which will be helpful for future superheavy experiments. We are also able to calculate the values of compound nucleus formation  $P_{\text{CN}}$  and survival  $P_{\text{surv}}$  probabilities, which suggest research in the right direction. We show here that  $\Delta R$  can be used to study every type of nucleus, whether the nuclei are heavy or superheavy or fissioning or nonfissioning. This unique feature makes the DCM remarkable in the field of theoretical models.

*Acknowledgments.* S.C. thanks the late Prof. Dr. Raj Kumar Gupta for training, guidance, and mentorship. The authors thank Prof. Dr. Horst Stöcker for his encouragement and useful critique of this work. P.H.O. acknowledges financial support from “Dirección General de Asuntos del Personal Académico UNAM,” PAPIIT-DGAPA (IN100421). S.C. acknowledges support as a guest scientist under a Humboldt fellowship at FIAS.

- [1] G. Adamian, N. Antonenko, W. Scheid, and V. Volkov, *Nucl. Phys. A* **627**, 361 (1997).
- [2] G. Adamian, N. Antonenko, W. Scheid, and V. Volkov, *Nucl. Phys. A* **633**, 409 (1998).
- [3] J. Hong, G. Adamian, and N. Antonenko, *Phys. Lett. B* **764**, 42 (2017).
- [4] Z.-H. Liu and J.-D. Bao, *Phys. Rev. C* **83**, 044613 (2011).
- [5] T. Matsuse, C. Beck, R. Nouicer, and D. Mahboub, *Phys. Rev. C* **55**, 1380 (1987).
- [6] S. J. Sanders, D. G. Kovar, B. B. Back, C. Beck, B. K. Dichter, D. Henderson, R. V. F. Janssens, J. G. Keller, S. Kaufman, T.-F. Wang, B. Wilkins, and F. Videbaek, *Phys. Rev. Lett.* **59**, 2856 (1987).
- [7] R. K. Gupta, S. K. Arun, R. Kumar, and Niyti, *Int. Rev. Phys. (IREPHY)* **2**, 369 (2008).
- [8] R. K. Gupta, in *Clusters in Nuclei, Vol. I*, edited by C. Beck, *Lecture Notes in Physics* Vol. 818 (Springer-Verlag, Berlin, 2010), pp. 223–265, and earlier references therein.
- [9] R. K. Gupta, in *Nuclear Particle Correlations and cluster Physics*, edited by W. U. Schröder (World Scientific, Singapore, 2016), pp. 471–497.
- [10] S. Chopra, M. K. Sharma, P. O. Hess, Hemdeep, and NeetuMaan, *Phys. Rev. C* **103**, 064615 (2021).
- [11] S. Chopra, N. Goel, M. K. Sharma, P. O. Hess, and Hemdeep, *Phys. Rev. C* **106**, L031601 (2022).
- [12] P. Lichtner, D. Drechsel, J. Maruhn, and W. Greiner, *Phys. Lett. B* **45**, 175 (1973).
- [13] J. Maruhn and W. Greiner, *Phys. Rev. Lett.* **32**, 548 (1974).
- [14] H. J. Fink, J. Maruhn, W. Scheid, and W. Greiner, *Z. Phys.* **268**, 321 (1974).
- [15] R. K. Gupta, W. Scheid, and W. Greiner, *Phys. Rev. Lett.* **35**, 353 (1975).
- [16] J. Maruhn and W. Greiner, *Z. Phys.* **251**, 431 (1972).
- [17] W. D. Myers and W. J. Swiatecki, *Ark. Fiz.* **36**, 343 (1967).
- [18] V. M. Strutinsky, *Nucl. Phys. A* **95**, 420 (1967); **122**, 1 (1968).
- [19] S. Chopra, M. Bansal, M. K. Sharma, and R. K. Gupta, *Phys. Rev. C* **88**, 014615 (2013).
- [20] A. Kaur, S. Chopra, and R. K. Gupta, *Phys. Rev. C* **90**, 024619 (2014).
- [21] S. Chopra, A. Kaur, and R. K. Gupta, *Phys. Rev. C* **91**, 034613 (2015).
- [22] S. Chopra, Hemdeep, and R. K. Gupta, *Phys. Rev. C* **95**, 044603 (2017).
- [23] S. Chopra, M. K. Sharma, P. O. Hess, and J. Bedi, *Phys. Rev. C* **105**, 014610 (2022).
- [24] Hemdeep, S. Chopra, A. Kaur, and R. K. Gupta, *Phys. Rev. C* **95**, 014609 (2017).
- [25] B. B. Singh, M. K. Sharma, and R. K. Gupta, *Phys. Rev. C* **77**, 054613 (2008).
- [26] Niyti, R. K. Gupta, and W. Griener, *J. Phys. G: Nucl. Part. Phys.* **37**, 115103 (2010).
- [27] R. K. Gupta, Niyti, M. Manhas, S. Hofmann, and W. Greiner, *Int. J. Mod. Phys. E* **18**, 601 (2009).
- [28] Niyti, R. K. Gupta, and P. O. Hess, *Nucl. Phys. A* **938**, 22 (2015).
- [29] G. Sawhney, G. Kaur, M. K. Sharma, and R. K. Gupta, *Phys. Rev. C* **88**, 034603 (2013).